EUROPEAN ORGANIZATION FOR NUCLEAR RESEARCH
CERN – AB DIVISION

CERN–AB–2003–052 ATB

A High Energy Secondary Beam of Ion Fragments for Instrumental Tests at CERN

M. Buénerd,
Laboratoire de Physique Subatomique et de Cosmologie
IN2P3/CNRS, 53 Av. des Martyrs, 3806 Grenoble-CEDEX, France

I. Efthymiopoulos
AB Division, CERN

Abstract

The design principle of a multi-ion beam for instrumental tests, based on the fragmentation of a primary ion beam, is described. This process is expected to provide secondaries with the same momentum per nucleon as the incident beam, and a variable range of nuclear elements in the beam, with the broadest distribution of charge Z extending for one particular setting of the transport line from $Z = 1$ up to $Z \approx$ 40-50 at most, with comparable individual rates on the average, for any heavy ion ($Z >\approx 50$) primary beam. The application in a secondary beam obtained from a 20 GeV/c per nucleon primary Pb ions at CERN is reported. The measured results are discussed.

Geneva, Switzerland

29 April 2003

1 Introduction

In a variety of experimental situations, the availability of a general purpose multi-ion beam is highly desirable. This applies to situations where the response of single detectors like silicon microstrip detectors, scintillators, or calorimeters, to ions over a range of nuclear mass is needed. This is particularly useful for instrumental tests related to isotope identification (ID).

This note reports on the development of a multi-ion secondary beam containing a variable range of nuclear masses, produced by projectile fragmentation on a nuclear target. The next section describes the basics of the magnetic filtering of the fragmentation yield and of the beam population. Section 3 provides a reminder of the Physics of the ion production mechanism implemented in the project, and proceeds with the evaluation of the secondary beam intensities that could be expected for standard primary beam conditions. Section 4 reports on the application of this principle to the case of a 20 GeV/c per nucleon beam of Pb ions incident in a Be target at CERN. The note is briefly concluded after some other possible applications have been quoted.

The multi-ion beam described in this note has been developed and used for the testing of the AMS RICH prototype at the H8 beam line in the North experimental area of the SPS [1] (see [2] for ealier results).

2 Beam production and ion mass spectrum

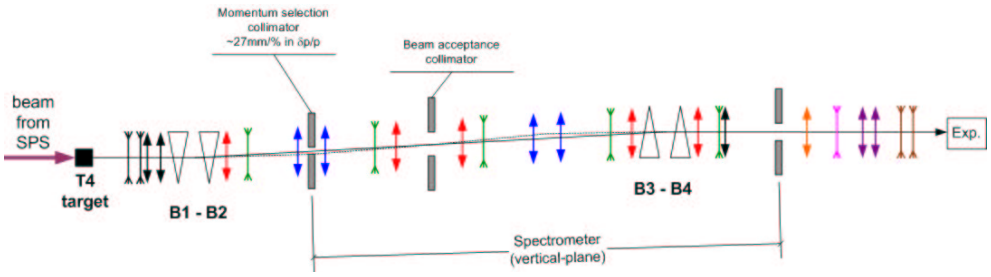

Figure 1: *Schematics of the H8 SPS North Area beam line used at CERN for fragment production and transport.*

The basic principle of the beam generation and transport system is of the same type as used at all accelerator facilities for secondary beam production. It is illustrated schematically on Figure 1. In the present case, a heavy ion beam is used to bombard the production target T4. Inside the target material, incident ions undergo nuclear fragmentation in peripheral collisions with target nuclei, with a

large cross section. The latter represents roughly one half or more of the total reaction cross-section depending on the system in collision and on the incident energy [3, 4], as described in the next section. A main kinematical feature of the produced particles is that the incident beam velocity is conserved by the fragments, with only a minor spread of a few percents (see [5] for example) induced by the collision dynamics. A fraction of the fragmentation products is transported into a beam line where particles are momentum analyzed by a combination of dipole magnets. The line will transport to the detectors only those particles which have the same rigidity, namely, $B\rho = 3.33P/Z$ with $B\rho$ in Tesla.meters set by the beam line optics, and the particle momentum P in GeV/c, Z being the charge of the particle (in proton charge units). For the energies of interest here, the momentum can be written at the relativistic limit as $P = \gamma M$, γ being the Lorentz factor of the particle and M its mass, which can itself be written in terms of the atomic mass number A times the atomic mass unit (1 amu=0.931 GeV). Finally the rigidity relation reads approximately as:

$$B\rho \approx 3.1\gamma\frac{A}{Z} \tag{1}$$

Since the fragmentation products fly to a good approximation at the beam velocity γ_b, only those particles entering the beam line with a ratio A/Z matching the relation $B\rho = 3.1\gamma_b A/Z$ will be transported to the detector. The $B\rho$ value of the beam setting thus allows to select the desired A/Z of the transported fragments. This principle is well known in the experimental nuclear physics community, among magnetic spectrometer users [6]. For example, the most useful ratio A/Z=2 provides a secondary beam including the following nuclear masses: ^{2}H,^{4}He,^{6}Li,^{10}B,^{12}C,^{14}N,^{16}O,..,^{28}Si,...,^{40}Ca,...,^{52}Fe,..etc.., produced by projectile fragmentation. The population of A/Z=2 elements transported by the line is limited however towards large (A,Z) values by the nuclear stability domain (see section 3.3 below). Other more selective particular field settings can be used as well, picking a particular $A/Z \neq 2$ isotope ratio, as it will be seen further below. The selectivity of the beam line is limited however, by the natural momentum spread of the fragmentation process because of which the rigidity relation 1 above can be satisfied for a variation $\Delta(A/Z)$ matching the physical spread of the Lorentz factor $\Delta\gamma$ of the produced particles.

3 Physics principles and beam rates

The source of secondary particles considered in the design, is the projectile fragmentation cross section whose generic production mechanism lies in the soft (nuclear and Coulomb) inelastic peripheral collisions between projectile and target

nuclei which generates a strongly forward peaked angular distribution of fragments. The production yield is large since the fragmentation cross section drains a large part of the total reaction cross section [3, 4, 7, 8, 9].

Other production mechanisms can be considered for light nuclei. See the discussion in [10] for low energy light nuclear fragments production by the coalesence mechanism.

The fragmentation process is symmetric and, projectile or target or both collision partners, can fragment in the interaction, with the fragments basically conserving the incident beam velocity. The reaction mechanism has been extensively studied and experimentally observed to occur over a very wide range of incident energies from as low as 20 MeV per nucleon up to highly relativistic energies [4, 7, 9, 8].

3.1 Phenomenological context

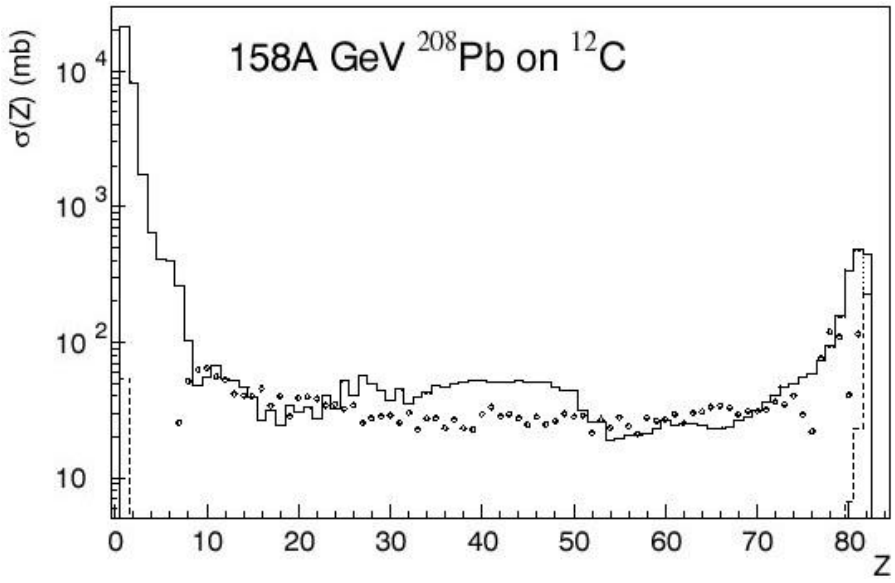

Figure 2: *Projectile fragmentation cross sections as a function of the nuclear charge of the fragments, measured recently for ^{208}Pb+^{12}C at 158 A GeV at the CERN SPS [4] (symbols) and theoretical results from ref [12] (histograms). Similar results are expected for 20 A GeV/c projectiles (see text).*

Figure 2 shows recent cross section data measured with nuclear track detectors [4] compared with the theoretical calculations of [12]. The data show that the fragmentation yield is of the same order of magnitude through the range of Z values extending from around 10 up to about 75. The calculations are in fair

agreement with this result. In addition, the same calculations predict large peaks of cross sections for very light nuclei and for projectile-like fragments. These latter features have been observed experimentally in several experiments [5, 7, 8, 9]. At very high energies, they correspond to a collision regime dominated by electromagnetic interactions (coulomb excitation).

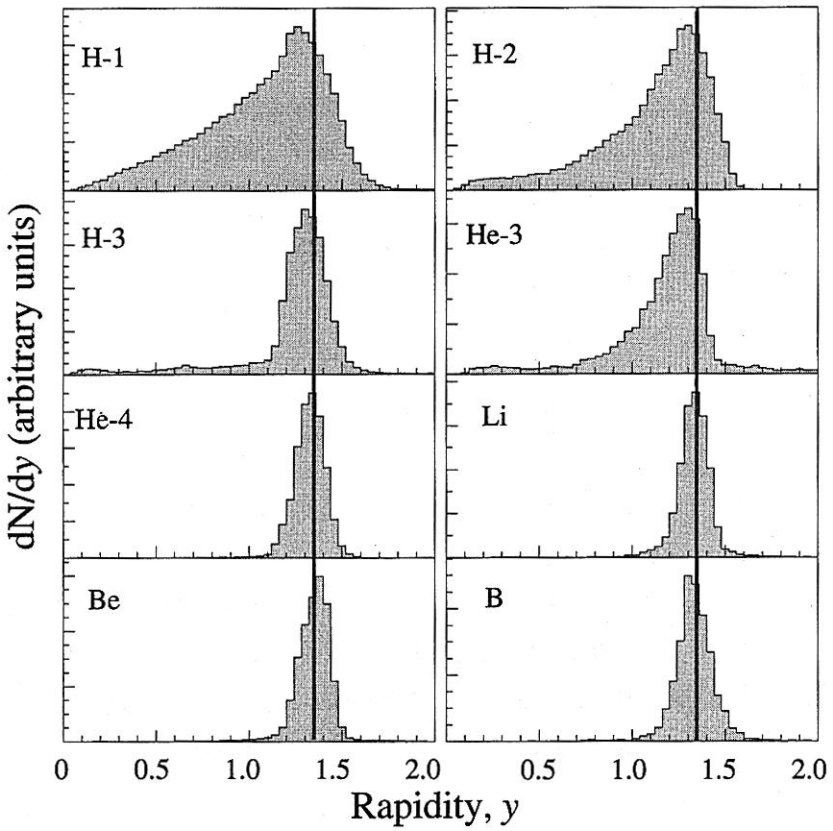

Figure 3: *Spectra of light nuclei produced by projectile fragmentation, measured in Au+C collisions at 1 GeV/n [5]. Note that the rapidity distributions of the fragments are all centered on the beam rapidity with very little spread around this value, especially for the heavier fragments shown on the figure. Note also the trailing low energy edge of the proton and light nuclei* $A < 3$*, distributions.*

The main features of the fragment momentum distributions are further illustrated on Figure 3, borrowed from ref [5], where the light fragment distributions produced in Au collisions on a carbon target at 1 GeV/n are shown to match the qualitative features expected from the fragmentation model [11]. Although this incident energy is much below those available at CERN, the same features are expected for the SPS energies since projectile fragmentation is a limiting process

which onset is known to take place at incident energies below 100 MeV/n incident energy.

3.2 Beam fragments rates

The rate of secondary beam fragment can be evaluated straightforwardly in the framework of the simple fragmentation model [11]. In this model, the fragments are produced by partition of the projectile based on a combinatorial grouping of the nucleons with a momentum spread induced by the Fermi momentum of the nucleons in the nucleus. The fragment rate transported in the beam line can be written (approximately) as:

$$n = N_i \frac{\sigma(F)}{\sigma_R} f(\frac{\delta P}{P}) f'(\Delta\Omega)\epsilon \tag{2}$$

Where N_i is the primary ion beam intensity (per spill of the SPS) $\sigma(F)$ and σ_R are the production cross section of the fragment F and the total reaction cross sections of the beam on the production target respectively, while $f(\frac{\delta P}{P})$ and $f'(\Delta\Omega)$ are the fractions of the momentum and angular distributions respectively (assuming that the factorisation assumption made here holds approximately), accepted in the transport line. P is the particle momentum and $\Delta\Omega$ the (mean) solid angle covered by the entrance slits of the beam line. The ϵ factor is the target acceptance. It will be taken as 1 for the coarse estimate made here. See below and Ref. [10] for the effect of the target thickness on the fragment mass distribution. As seen on Figure 2 and from ref [4], the fragment production cross section is of the order of 30-40 mb over the $8 \lesssim Z \lesssim 40$ range of nuclear charge. Assuming a primary beam intensity of 10^7 Pb particles per spill (12.54s) on the target, total reaction cross sections σ_R of 3200 mb and 8600 mb for Pb+Be and Pb+Pb respectively, and a thickness of ~ 0.25 proton interaction length for the production target, this roughly corresponds to rates of the order of 10^5 particles produced per spill and per nuclear element at the target. Note that the quoted target thickness corresponds to about 4 interaction lengths for Pb ions, which implies that all incident ions interact in the target.

The two fractions appearing in relation 2 above can be estimated as follows:

Momentum spread

In the fragmentation model [11] the momentum distribution of the produced fragments with mass M_f in the center of mass of the projectile, is gaussian with a rms value $\sigma(P_{lab}, A_p)$ depending on the fragment and projectile mass numbers A_f and A_p, and of the nuclear Fermi momentum: $\sigma^2 = \sigma_0^2 \frac{A_f(A_p - A_f)}{(A_p - 1)}$, with σ_0 being of the order of 90 MeV. Boosting the momentum to the lab frame and

taking into account the characteristic longitudinal momentum (P_l) spread of one σ_p (RMS) unit, one gets:

$$P_l^{lab}(M_f) = \gamma P_l^{proj}(M_f) + \beta\gamma E^{proj}(M_f) \approx \pm\gamma\sigma_p + \gamma M_f$$

Where the momentum spread appears thus to be of the order of $\sigma_0 \frac{\sqrt{A_f}}{M_f}$ in the present case for light nuclear fragments, i.e., of about 3%. This number is to be compared to the maximum momentum acceptance of the beam line of 1.5%. The fraction $f(\frac{\delta P}{P})$ above is thus a sizable fraction of unity.

Angular spread

The angular slope can be estimated on the same basis: The characteristic transverse momentum is $< p_t > \gtrsim \sigma$. The RMS angle of production of ^{12}C in the lab frame for example, is thus $\frac{\sigma}{P_{lab}} \approx \sigma_0 \frac{\sqrt{A_f}}{P_{lab}}$ ≈1.2 mrad for 20 GeV/n incident particles. It would be about one order of magnitude smaller at 158 GeV/n. Since the angular acceptance of the beam line is of the order of 1 mrad, the fraction $f'(\Delta\Omega)$ above is also not small compared to unity.

Taking conservative ansatz values of 0.1 for both f and f' leads to beam rates of the order 10^3 per spill for a given transported element. These numbers show that for usual needs of instrumentation testing, the expected beam rates are suitable. The experimental numbers are somewhat higher but in fair qualitative agreement with these values, as it will be seen below.

Note that the fragmentation products can interact again in the target according to their particular cross sections. The flux emerging from the target can be corrected by solving the corresponding transport equation. The relative flux rates between high and low Z fragments is decreasing with the increasing thickness of the target. For Fe/Li this ratio varies from about 10^{-2} for a 5 cm target down to about 2 10^{-3} for 30 cm [10].

3.3 Beam transport selectivity

As it was seen above, the projectile velocity conserving fragments are selected by the beam line according to their mass over charge ratios.

Fig. 4 shows the map of the nuclides, number of protons versus number of neutrons of the stable isotopes (with respect to strong interactions, most of them being β unstable). On this map the particles transmitted by the beam line to the experimental area are those lying along a line with a slope A/Z. For A/Z=2 as shown on the figure, it is seen that the selection line crosses the nuclear stability region between deuterium and Z ≈40-50. Beyond this range of Z, the selection line is out of the nuclear stability region, where no yield is expected. The transported fraction of the fragmentation yield will thus be limited to the range

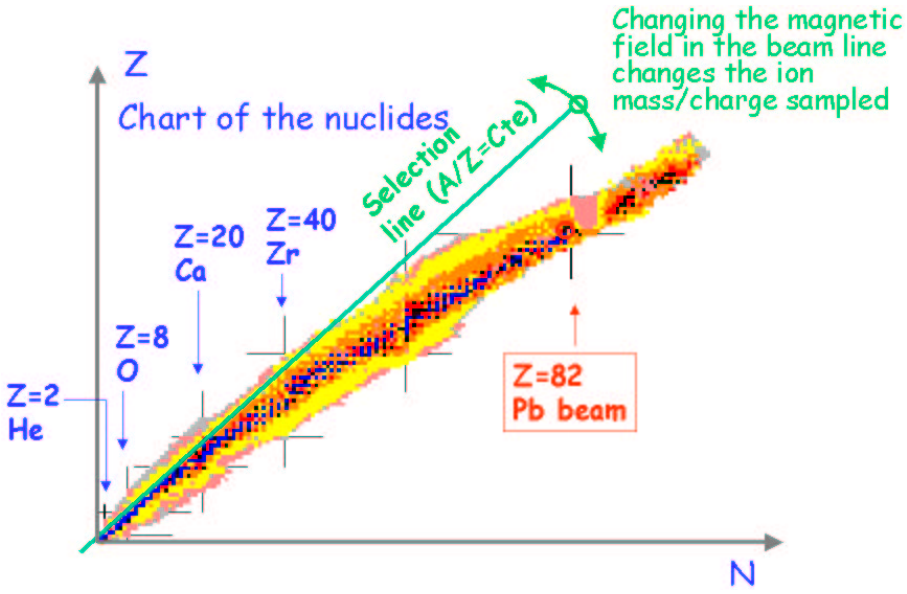

Figure 4: *Chart of the nuclides showing the distribution of stable nuclei with proton number Z versus neutron number N, and the line of isotope selection with slope A/Z =2 ($Z = N$).*

Z=1 to Z≈40 of nuclear elements with A/Z =2. The observed experimental limit seems to be even below this value (see fig 5). This was a very welcome feature for the instrumental tests of the AMS RICH for which the upper limit of the useful range was around Z=26 (Fe), higher Z values being an unwanted background.
Changing the rigidity settings of the transport line corresponds to changing the A/Z slope of the selection line in the map of nuclei of Fig. 4. This flexibility of the beam line selectivity is also useful for picking up some specific isotopes (see below). Fragments however, as it has been mentioned above, are produced with a momentum spread Δp_f with respect to the beam velocity. For those fragments whose corresponding spread of the Lorentz factor is $\Delta\gamma_f/\gamma_f > \Delta A/A$ for a given value of Z, the isotopes cannot be resolved. This is the case for light isotopes p,d and $^{3,4}He$ because of the large momentum spread.

3.4 Protons

As mentionned above, light fragments, in particular protons and deuterons, but also ^3He [5], have distributions trailing down to low momentum values. Protons in particular are produced through the whole range of rapidity kinematically allowed between the target and projectile rapidities (see Fig. 3). This could be

expected since protons are emitted in strongly dissipative central as well as in soft peripheral collisions.
This allows to have protons in the whole momentum range below the incident projectile momentum per nucleon, down to the lower momentum limit of the beam line.

4 The CERN beam of ion fragments

The above ideas have been implemented in the development of a 20 GeV/C per nucleon beam of secondary ions for the test of the AMS RICH prototype which results will be reported separately [1].
The run took place during the 2002 ion beam period at CERN. Fully stripped Pb ions [13] at 20 GeV/c per nucleon were used to bombard the SPS T4 (Be) target. The produced particles were transported over about 500 m in the H8 beam line to the experimental area (Fig 1). The devices to be tested were prototypes of the AMS RICH, tracker silicon microstrips, and time of flight hodoscope elements of the future AMS02 spectrometer.
The production target thickness and material used were 10 cm Be for the ion runs and 4 cm Pb for the proton runs ($A/Z = 1$ setting). The mean primary beam intensity at the target was of the order of $\sim 8 - 9 \times 10^7$ per spill. The maximum angular acceptance of the beam line was $d\Omega_{max} = 2.4\mu Sr$, and maximum momentum spread $\delta P/P \sim 1.5\%$ [14].
The observed trigger rates for the main ion settings used are given in the table. Note that the rates measured for the A/Z =2 settings roughly corresponds to the individual mean rates per elements observed for the other two settings, times about 50 elements transported for this configuration, which is about what was observed (see Figure 5).
For the proton runs, the beam momentum was varied over the set of following values: 5, 7, 9, 11, 13, 15, 20 (beam velocity), in GeV/c, for which the observed rates were: 240, 900, 2400, 5300, 1000, 2000, and 2500 protons per spill respectively. The increase of the rate at low momenta was expected. However, the rate maximum observed for the 11 GeV/c setting and the behaviour at larger momenta are not fully understood.

5 A Cosmic-Ray-like ion beam

Figure 5 compares the charge distribution of the transported nuclear species (A/Z$\sim$2), with the natural abundance spectrum of the CR elements from [15]. The former is the simple dE/dx energy loss spectrum measured by a beam

Table 1: *Mean rates of beam fragments measured for various rigidity settings of the beam line, per spill of the SPS for the beam conditions discussed in the text. The A/Z =2 rate indicated is a maximum value which was measured but not used during the tests.*

Beam Rigidity (GeV/c / charge)	A/Z	Isotopes	rate (for $\sim 10^7$ ions on target)
40	2	D to Zr region	$<1.3\ 10^5$
35	7/4	^{7}Be	$2.5\ 10^3$
30	3/2	^{3}He	$2.5\ 10^3$

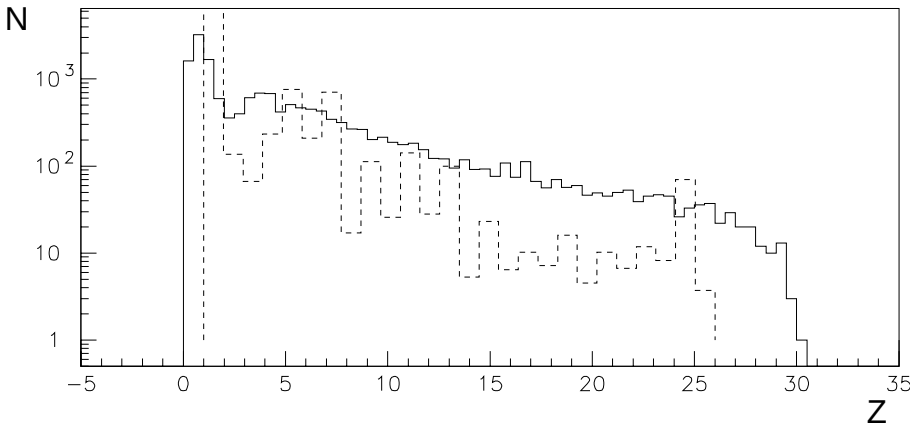

Figure 5: *Comparison of the charge spectrum of the beam, obtained from energy loss measurements by trigger scintillators (solid histogram), with the distribution of the Cosmic Ray abundance of elements (dashed histogram). The two distributions are put on the same horizontal scale of nuclear charge, approximately, and they look qualitatively very similar.*

(scintillator) counter [1]. The calibration is approximate, based on the known response of scintillators to ions.
It is interesting to note that the charge dependence of the beam elements exhibits a quite similar trend as the element distribution of the CR abundance. This is not totally surprising since it is known that the CR spectrum of light elements is largely populated by the ion fragmentation process, the initial conditions being however more than significantly different. Note however that this similarity concerns the charge distribution only. Since the mass A distribution is constrained by the A/Z =2 in the beam, the isotope distribution is necessarily very different form that of the CR spectrum. The case of Be (Z=4) is very illustrative of this limitation as an extreme situation. Since ^{8}Be is not a stable nuclide, the corresponding yield of this element for the A/Z =2 setting, is basically absent from the beam population, while the stable isotopes $^{7,9}Be$ are normally abundant in CRs.
Among the interesting measurements which could be performed with such a test beam is the identification capability of Be isotopes in the perspective of ^{10}Be abundance measurements in CRs, which provides a measurement of the time of confinement of CRs in the galaxy [16]. This could be potentially be achieved with beam ions within the appropriate range of incident velocity and with the appropriate A/Z beam line settings to select this isotope or at least enhance the beam population for this isotope.
Nevertheless, this comparison shows that such a composite ion beam provides a quasi-CR element distribution which is potentially interesting for investigating the response of instruments to be embarked on satellites for CR measurements. Since the individual element rates are of the order of 2.5 10^3 per ($\sim$12.5 s) spill on the average, and since the natural flux of carbon ions is of the order of 10 s^{-1}, the beam used here offers a time boost of about 10 for long duration tests of CR equivalent conditions. Although modest, this prospect may be interesting for future payloads.
Finally, it may also be interesting to note that such an experimental arrangement could also be used as well for physics measurements of the fragmentation cross sections, in which the beam line is used as a magnetic spectrometer, measuring the fragmentation yield of isotopes in counter experiments at (ultra) relativistic energies on a thin target as was done already by the NA49 and (mainly) NA52 experiments.

6 Summary and conclusion

A 20 GeV/c per nucleon secondary (multi)ion beam has been developped at CERN with some flexibility in the ion selectivity. The ion population for the

main beam includes all ions with A/Z =2 between deuterium and the region Z$\sim$40. Count rates of about 2.5 10^3 particles per element per spill of the SPS have been obtained for elements with Z$>$2. The element distribution of the beam is similar to that of the natural abundance distribution of the Cosmic Ray spectrum.

References

[1] The AMS-RICH collaboration, M. Buénerd et al., Proc. ICRC 2003 Conf., Tsukuba (Japan), July 31-Aug 7, 2003, to be published; and The AMS-RICH collaboration, in preparation for NIM A.

[2] T. Thuillier et al., Nucl. Inst. and Meth. in Phys. A491(2002)83

[3] Y.D. He and P.B. Price, Z. Phys. A 348(1994)105

[4] S. Cecchini et al., Nucl. Phys. A 707(2002)513

[5] J.A. Hauger et al., Phys. Rev. C57(1998)764

[6] See for example, G. Blank et al., Nucl. Inst. and Meth. in Phys. A491(2002)83; A.C. Mueller and B.M. Sherrill, Ann. Rev. Nucl. Sci. 43(1993)529; A. Joubert et al., GANIL reports A-91-01, June 1991 and P-93-04, Aug. 1993.

[7] C.K. Gelbke et al., Phys. Rep. 42(1978)311

[8] A.S. Goldhaber and H.H. Heckman, Ann. Rev. Nucl. Sci. 28(1978)161

[9] J. Mougey et al., Phys. Lett. B 105(1981)25

[10] M. Buénerd, L. Derome, R. Duperray, and K. Protasov, Internal AMS note 2002-05-02

[11] A.S. Goldhaber, Phys. Lett. B 53(1974)306

[12] C. Scheidenberger, I.A. Pshenichnov, K. Sümmerer, submitted to Phys Rev C, and private communication; see also K. Sümmerer and B. Blank, nucl-ex/9911006.

[13] SL Annual Report for the Year 2002, M. Meddahi, AB-Note-2003-018 ATB

[14] SPS Experimenters' Handbook, 1981; P. Coet and N. Doble, CERN/SPS/86-23 (EBS), 1986.

[15] J.A. Simpson, Ann. Rev. Nucl. and Part. Sci. 33,323 (1983)

[16] A. Bouchet et al., Nucl. Phys. A688(2000)417c.